IVYSPRING INTERNATIONAL PUBLISHER

Journal of Cancer

2017; 8(15): 3078-3085. doi: 10.7150/jca.20250

Research Paper

Hyperpolarized ^{13}C Diffusion MRS of Co-Polarized Pyruvate and Fumarate to Measure Lactate Export and Necrosis

Benedikt Feuerecker[1, 5]✉, Markus Durst[2, 3], Michael Michalik[1], Günter Schneider[4], Dieter Saur[4, 5], Marion Menzel[3], Markus Schwaiger[1], Franz Schilling[1]

1. Department of Nuclear Medicine, Klinikum rechts der Isar, Technische Universität München, Munich, Germany;
2. Institute of Medical Engineering, Technische Universität München, Garching, Germany;
3. GE Global Research, Munich, Germany;
4. Department of Internal Medicine II, Klinikum rechts der Isar, Technische Universität München, Garching, Germany;
5. German Cancer Consortium (DKTK) and German Cancer Research Center (DKFZ), Heidelberg, Germany.

✉ Corresponding author: benedikt.feuerecker@tum.de, Tel: 0049-89-4140-4558

© Ivyspring International Publisher. This is an open access article distributed under the terms of the Creative Commons Attribution (CC BY-NC) license (https://creativecommons.org/licenses/by-nc/4.0/). See http://ivyspring.com/terms for full terms and conditions.

Received: 2017.03.24; Accepted: 2017.06.04; Published: 2017.09.02

Abstract

Background: Non-invasive tumor characterization and monitoring are among the key goals of medical imaging. Using hyperpolarized ^{13}C-labelled metabolic probes fast metabolic pathways can be probed in real-time, providing new opportunities for tumor characterization. In this *in vitro* study, we investigated whether measurement of apparent diffusion coefficient (ADC) measurements and magnetic resonance spectroscopy (MRS) of co-polarized ^{13}C-labeled pyruvic acid and fumaric acid can non-invasively detect both necrosis and changes in lactate export, which are parameters indicative of tumor aggressiveness.

Methods: ^{13}C-labeled pyruvic acid and fumaric acid were co-polarized in a preclinical hyperpolarizer and the dissolved compounds were added to prepared samples of 8932 pancreatic cancer and MCF-7 breast carcinoma cells. Extracellular lactate concentrations and cell viability were measured in separate assays.

Results: The mean ratios of the ADC values of lactate and pyruvate (ADC_{lac}/ADC_{pyr}) between MCF-7 (0.533 ± 0.015, n = 3) and 8932 pancreatic cancer cells (0.744 ± 0.064, n = 3) showed a statistically significant difference ($p = 0.048$). 8932 cells had higher extracellular lactate concentrations in the extracellular medium (22.97 ± 2.53 ng/µl) compared with MCF-7 cells (7.52 ± 0.59 ng/µl; $p < 0.001$). Fumarate-to-malate conversion was only detectable in necrotic cells, thereby allowing clear differentiation between necrotic and viable cells.

Conclusion: We provide evidence that MRS of hyperpolarized ^{13}C-labelled pyruvic acid and fumaric acid, with their respective conversions to lactate and malate, are useful for characterization of necrosis and lactate efflux in tumor cells.

Key words: Hyperpolarization, diffusion-weighted magnetic resonance spectroscopy, lactate export, tumor metabolism.

Introduction

Since Warburg's discovery, that solid tumors intensely metabolize glucose, glycolysis as a key metabolic pathway has been used for cancer diagnosis. A glycolytic phenotype is present in most human cancers and can therefore be used for imaging, e.g. by ^{18}F-FDG-positron emission tomography. In tumor cells this elevated glucose turnover results in the accumulation of lactate, resulting in increased lactate concentrations in both intra- and extratumoral space, the latter resulting in an acidification of the tumor microenvironment [1-3]. Magnetic resonance spectroscopic (MRS) imaging using hyperpolarized

^{13}C-labelled metabolic probes is a new imaging modality which can be used to probe fast metabolic pathways in real time [4]. Although the metabolites' distribution in intra- or extracellular compartments is unclear, it is largely influenced by the expression of proton-linked monocarboxylate transporters (MCT). For mammalian MCT transporters proton-linked pyruvate and lactate transport was demonstrated for the transporters MCT 1-4 [5, 6]. These transporters are involved in a number of metabolic pathways that are crucial for the maintenance of cellular homeostasis such as import and efflux of lactate into the intra- and extracellular space [5]. MCT 4 transporters are up-regulated in hypoxic cancer cells that release lactate to the microenvironment [5-9]. Such an increase of lactic acid efflux is an important biomarker of tumor aggressiveness and metastatic potential, and is therefore an important target for molecular imaging [10-13].

Using hyperpolarized pyruvate as a substrate allows monitoring the exchange of the hyperpolarized carbon label on carbon position 1 of pyruvate with lactate. The rate of this process is determined by lactate dehydrogenase (LDH) concentration, LDH activity, NAD^+/NADH levels and the metabolites' pool sizes [14]. In order to differentiate intra- from extracellular signals the different diffusion behaviors of metabolites from different compartments can be used for separation, since the diffusion coefficient of metabolites located in the separate cellular compartments can vary up to 10-fold [15]. Other approaches involve Gadolinium (Gd)-based compounds that have been designed to quench the extracellular compartment or to specifically bind to intracellular structures in order to allow compartmental differentiation [16-19]. As shown previously, the intracellular apparent diffusion coefficient (ADC) is lower than the extracellular ADC due to diffusion restriction inside the cell [20-22]. There is evidence that diffusion NMR and MRI can provide information about the metabolites' microenvironment as well as about the intactness of the plasma membrane (grade of necrosis). Therefore, such techniques may allow also judgments about therapy response [4].

In this study, we show that diffusion-weighted magnetic resonance spectroscopy (MRS) of hyperpolarized ^{13}C-labelled pyruvic acid, fumaric acid, lactate and malate is useful to measure lactate export and necrosis.

Methods

Hyperpolarization and NMR measurements

A polarization mixture was prepared containing frozen layers of 4 µl of a solution of 14 M [1-^{13}C]pyruvic acid (Cambridge Isotope Laboratories, Andover, MA, USA), 15 mM OX063 trityl radical (Oxford instruments, Abingdon, Oxfordshire, UK), 1 mM Dotarem (Guerbet, Villeprinte, France) and 12.5 µl of a mixture of 4 M [1,4-$^{13}C_2$]fumarate in dry DMSO, 27 mM OX063 trityl radical (Oxford instruments, Abingdon, Oxfordshire, UK) and 2.5 mM Dotarem (Guerbet, Villeprinte, France) [23]. For each polarization experiment this mixture was loaded into a HyperSense polarizer (Oxford Instruments), operating at a magnetic field of ~ 3.35 T, temperature of ~ 1.4 K, microwave frequency of ~ 94.1 GHz and microwave power of ~ 100 mW, and polarizer for ~ 40 min. The polarized sample was rapidly dissolved with ~ 5 mL of a dissolution agent consisting of 30 mM NaOH, 30 mM tris(hydroxymethyl)amino-methane (TRIS) buffer and 12.5 mg/L disodium ethylenediaminetetraacetate (Na_2EDTA) in D_2O (temperature, ~ 185 °C; pressure, ~ 10 bar). The final solution contained 11.2 mM hyperpolarized [1-^{13}C]pyruvate and 10 mM [1,4-$^{13}C_2$]fumarate at 37 °C with pH ~ 7.4 and liquid-state polarization of ~ 25%, which was monitored in a Minispec mq NMR analyzer (Bruker Optik, Ettlingen, Germany) operating at 0.94 T.

As the hyperpolarized sample had to be transported to another building, magnetization losses caused by T_1 relaxation had to be minimized to maintain hyperpolarization. T_1 of pyruvate was increased from ~ 68 s (dissolution in H_2O, 35 °C) to ~ 165 s (dissolution in D_2O, 45 °C) at a field strength of 0.94 T, as a result of decreased dipolar relaxation from both deuterated solvent and increased temperature [4]. Measurements of the pyruvate T1 were performed using a constant flip angle pulse-acquire sequence in a Minispec mq40 NMR analyzer (Bruker Optik, Ettlingen, Germany) operating at 0.94 T. After dissolution, the sample was attached to a preheated (45 °C) 0.5 T permanent magnet whilst being transported the 0.5 km distance by bicycle to a 14.1 T AvanceIII microimaging system (Bruker BioSpin, Rheinstetten, Germany). It is equipped with a 10-mm (inner diameter) water-cooled micro5-probehead supporting gradient strengths up to 3 T/m. We used an 8-mm double-tuned ^{1}H-^{13}C coil insert. The transport time was 100 s, which lead to a signal decay of around 50% of the pyruvate in the D_2O solution. An aliquot (0.2 mL) of the pyruvate-fumarate-D_2O solution was injected into an 8-mm susceptibility-matched NMR glass tube (susceptibility plug, Doty Scientific, Inc. Columbia, SC, USA) containing 0.8 mL of a tumor suspension (~ 20-40 x 10^6 8932 pancreatic or MCF-7 tumor cells) in assay medium.

Hyperpolarized diffusion-weighted NMR spectroscopy

A diffusion-weighted pulsed gradient spin echo (PGSE) sequence was used for the measurement of ADCs of hyperpolarized ^{13}C-labelled nuclei. For a detailed description of the sequence design and about the choice of experimental parameters please refer to the paper from Schilling *et al*. [4]. In the current study, we used a repetition time of 1 s, an acquisition time of 0.5 s, a flip angle of 30˚, diffusion time Δ = 40 ms, diffusion gradient time δ = 2 ms, and diffusion gradient strength = [0, 180, 150, 0, 120, 90, 0, 60, 30, 0, 0, 0, 0, 0] G/cm corresponding to a maximum *b*-value of 2.3 ms/mm^2.

Data analysis

Since tumor cells received a high concentration of pyruvate, leading to saturation and a signal intensity ~ 40-fold higher than that of lactate. Changes in pyruvate signal due to exchange of the hyperpolarized label from lactate with pyruvate was found to have a negligible effect on the signal intensities and was therefore neglected. Metabolite signals below the noise-level, mostly occurring for lactate at high *b*-values due to the low metabolite concentration, were not included in the data analysis. ADCs of pyruvate, fumarate and lactate were modeled by the standard Stejskal-Tanner signal equation [4] and were corrected for flip angle and T_1 times as described by:

$$I_g(b,t) = I_0 \exp\left(\frac{-t}{T_{1,eff}}\right) \exp(-bD) = I_0 \exp\left(\frac{-t}{T_{1,eff}}\right) \exp\left[-\left(\Delta - \frac{\delta}{4}\right)\left(\frac{2\gamma g \delta}{\pi}\right)^2 D\right]$$

where I_0 is the initial signal at t = 0 s, γ is the gyromagnetic ratio of carbon, *D* denotes the ADC and *b* is the amount of diffusion sensitivity by the magnetic field gradients (*b*-value) [4, 24]. The effective T_1 ($T_{1,eff}$) values for pyruvate and lactate were calculated for *b* = 0 values and fitted accordingly using a monoexponential fit. Table 1 displays the $T_{1,eff}$ values (overall) of 3.73 ± 0.13 seconds for pyruvate and 4.50 ± 0.24 seconds for lactate.

Table 1. displays the effective T_1 ($T_{1,eff}$) values [s] of lysed (cells that were treated with Triton X-100) and normal, untreated cells. No statistical differences were detected between groups indicating the robustness of the measurements regardless of the status in which the cells are.

Mean ± SD	Pyruvate $T_{1,eff}$ [s]	Lactate $T_{1,eff}$ [s]
Overall (n = 11)	3.73 ± 0.13	4.50 ± 0.24
lysed cells (n = 3)	3.88 ± 0.12	4.27 ± 0.17
Normal cells (n = 8)	3.58 ± 0.31	4.73 ± 0.50

Signal assignments were performed according to literature whereas assignments were the following [25-27]: [1-^{13}C] pyruvate (171 ppm), [1-^{13}C] lactate (183 ppm), [1,4-$^{13}C_2$] fumarate (≈ 175 ppm), [1-^{13}C] pyruvate hydrate (≈ 179 ppm), [1-$^{13}C_2$] malate (≈ 182 ppm) and [4-$^{13}C_2$] malate (≈181 ppm).

MCF-7 breast cancer and 8932 pancreatic tumor cells

The human breast cancer cell line MCF-7 (ATCC® HTB-22™) was cultivated as a monolayer in Dulbecco's modified Eagle's medium (DMEM Biochrom, Germany) supplemented with 5% fetal calf serum (37 °C, 5% CO_2). The mouse pancreatic tumor cell line 8932 was maintained as a monolayer culture in Dulbecco's modified Eagle's medium (DMEM Biochrom, Germany) supplemented with 10% fetal calf serum (FCS) and 1% Penicillin/Streptomycin (Pen/Strep, Biochrom, Germany). This cell line was established from the pancreatic cancer of a *Ptf1a$^{Cre/+}$;LSL-PIK3CA$^{H1047R/+}$* mouse as previously described [28, 29]. The cells were detached immediately before the NMR measurement with Trypsin/EDTA and centrifuged at 1300 rpm for 3 min. The cell pellet was dissolved in DMEM (supplemented with 10% FCS and 1% Pen/Strep) and transferred to an 8-mm susceptibility-matched NMR glass tube. The cell number was determined using a Neubauer cell counting chamber. For delineation of dead cells the solution of cells was stained with Trypan blue. Cell numbers were ~ 20-40 x 10^6. To investigate the diffusion characteristics of tumor cells undergoing membrane changes, 8932 tumor cells were incubated with 0.002% Triton X-100 in the assay medium**.** At this concentration of Triton X-100, membrane permeabilization was an immediate process over several seconds, as tested in a preceding experiment with trypan blue staining.

Viability/proliferation of 8932 pancreatic cancer cells and MCF-7 tumors cells

Viability/proliferation of 8932 pancreatic cancer cells and MCF-7 breast cancer cells was evaluated using a WST-1 proliferation assay (Roche Diagnostics). For quantification 2.5 x 10^3 cells were seeded in triplicates in 96-well plates and were left to adhere overnight. Metabolic activity of cells, indicative of cell proliferation/viability, was assessed after addition of 10 µl (per 100 µl medium) of a liquid reagent containing tetrazolium salt to the respective cell medium. Changes in formazan dye generation were measured in an ELISA reader after 30 min of incubation at 37°C and 5% CO_2 (Bio-Tek ELISA Reader EL 800, Bio-Tek Instruments GmbH, Bad Friedrichshall, Germany). Results of absorbance

measurements (450 nm) of both cell lines were plotted in one graph to display relative metabolic activity of both cell lines.

Determination of the lactate concentration in cell supernatant

To determine the concentration of lactate in the supernatant of the MCF-7 and 8932 tumor cells, the cell medium was collected following adhesion of the cells overnight at 37 °C and 5 % CO_2. To evaluate the effects of addition of the hyperpolarized ^{13}C pyruvic acid on the cells, pyruvic acid at a concentration of 100 mM was prepared in the respective medium. Cell medium was discarded and replaced with the pyruvic acid containing medium. Supernatant was collected 30s after addition of the pyruvic acid containing medium. The amount of extracellular lactate was determined using a commercially available assay (Lactate Assay Kit, Sigma-Aldrich), which uses an enzymatic conversion that results in a colorimetric product that is proportional to the lactate in the sample. Preparation of the analysis was done according to the manufacturers' instructions and extinction was measured with an ELISA reader at 570 nm (Bio-Tek ELISA Reader EL 800, Bio-Tek Instruments GmbH, Bad Friedrichshall, Germany). Experiments were carried out in triplicates. The lactate concentration in the samples was calculated based on a standard curve of known lactate samples and is displayed in ng/µl.

Statistical methods

Statistical analysis was performed using Graph Pad Prism (version 4.0, GraphPad Software, Inc.). Means and standard deviations were calculated from at least three independent experiments. A *t*-test was used to compare means of two independent samples. The level of statistical significance was set at $p < 0.05$. Beyond, an ANOVA analysis was used for to analyze differences among group means.

Results

^{13}C-diffusion coefficients of live and dead tumor cells

8932 and MCF-7 tumor cells in culture medium were analyzed following their transfer to an 8 mm NMR tube and 20 s after injection of the hyperpolarized compound. Twenty seconds after injection of hyperpolarized [1-^{13}C]pyruvate and [1,4-$^{13}C_2$]fumarate, diffusion-weighted spectra were acquired within 120 s. Pyruvate, lactate, fumarate, and malate signals were measured at a linewidth of 15 Hz, allowing for a good separation of signals.

^{13}C metabolite ADCs of viable cells could be calculated for pyruvate, fumarate and lactate (Figure 1A), the latter originating in the cells. Exemplary spectra are shown in Fig. 1D. Statistical analysis revealed a significant difference ($p = 0.048$) in the mean values of ADC_{lac}/ADC_{pyr} between MCF-7 (0.533 ± 0.015, n = 3) and 8932 cells (0.744 ± 0.064, n = 3) as shown in Figure 1B. As displayed in Figure 2, also differences in lactate/pyruvate ratios were observed with regard to the cell type and treatment regimen (0.053 ± 0.035 for MCF-7 cells, 0.0869 ± 0.031 for 8932 cells, and 0.011 ± 0.006 for necrotic 8932 cells). Following treatment with Triton X-100 a statistically significant decrease in the lactate/pyruvate ratio in 8932 cells was noticed compared with untreated 8932 cells. Upon lysis with Triton X-100 in 8932 cells NMR spectra showed two additional peaks, which correspond to the respective peaks of malate (Figure 1D, inset figure). Malate was only observed in necrotic cells whereas lactate could only be detected in viable cells, thereby allowing a clear differentiation.

Lactate concentration in cell supernatant

The assessment of lactate concentrations as measured by colorimetric generation of detectable products relative to lactate concentration within the supernatant of 8932 pancreatic cancer cells and MCF-7 breast cancer cells revealed that 8932 cells showed higher extracellular lactate concentrations after addition of a 100 mM pyruvate solution (T 30) in the extracellular medium (22.97 ± 2.53 ng/µl) compared with MCF-7 cells (7.52 ± 0.59 ng/µl). Statistical significance was achieved in the second time point ($p < 0.001$). Base levels of lactate (T 0) as determined by collection of the supernatant showed no differences between cell lines (8932: 3.83 ± 0.38 ng/µl, MCF-7: 3.77 ± 0.16 ng/µl; Figure 3A).

Viability/proliferation of 8932 pancreatic cancer cells and MCF-7 tumors cells

Pancreatic cancer cells 8932 showed a higher absorbance compared with MCF-7 tumor cells as displayed in Figure 3B. Since higher absorbance correlates with an augmentation of formed formazan dye, higher absorbance point to increased metabolic activity of these cells. Our results showed that 8932 cells had a approx. 11 times higher absorbance compared with MCF-7 cells. (8932: 2.07; MCF-7: 0.19; $p < 0.0001$).

Discussion

In this study, we investigated the use of hyperpolarized ^{13}C-labelled pyruvate and fumarate in combination with diffusion measurements to discriminate viable from necrotic cells and to assess lactate export in two different cell lines. We have linked the ADC ratio of lactate to pyruvate

ADC_{lac}/ADC_{pyr} to the relative compartmental distribution of lactate in the intra- and extracellular compartment. Indirectly, this serves as a measure of lactate export, since accumulation of lactate after rapid export from within the cell results in an increase in ADC_{lac}/ADC_{pyr}.. Because ADC_{lac}/ADC_{pyr} ratios can also be affected by cell viability [4], co-polarization of fumarate was established as a simultaneous, independent and unambiguous assessment of necrosis.

The need for non-invasive imaging markers becomes evident in the light of treatment response evaluation after cancer treatment with new anti-angiogenetic agents such as bevacizumab [30]. There is growing evidence that the follow-up imaging during and after the treatment with these agents cannot be appropriately carried out using e.g. the standard procedures such as the RECIST criteria based on Computer Tomography (CT) due to the lack of tumor shrinkage, pointing out an unmet demand for new imaging procedures that are able to provide new insight on the efficacy of tumor treatment. Using our bimodal approach including a functional imaging procedure with hyperpolarized ^{13}C-labeled compounds that reveals functional status and simultaneously makes use of diffusion properties, which uncover compartmental discrimination, could be a valuable tool in such a setting.

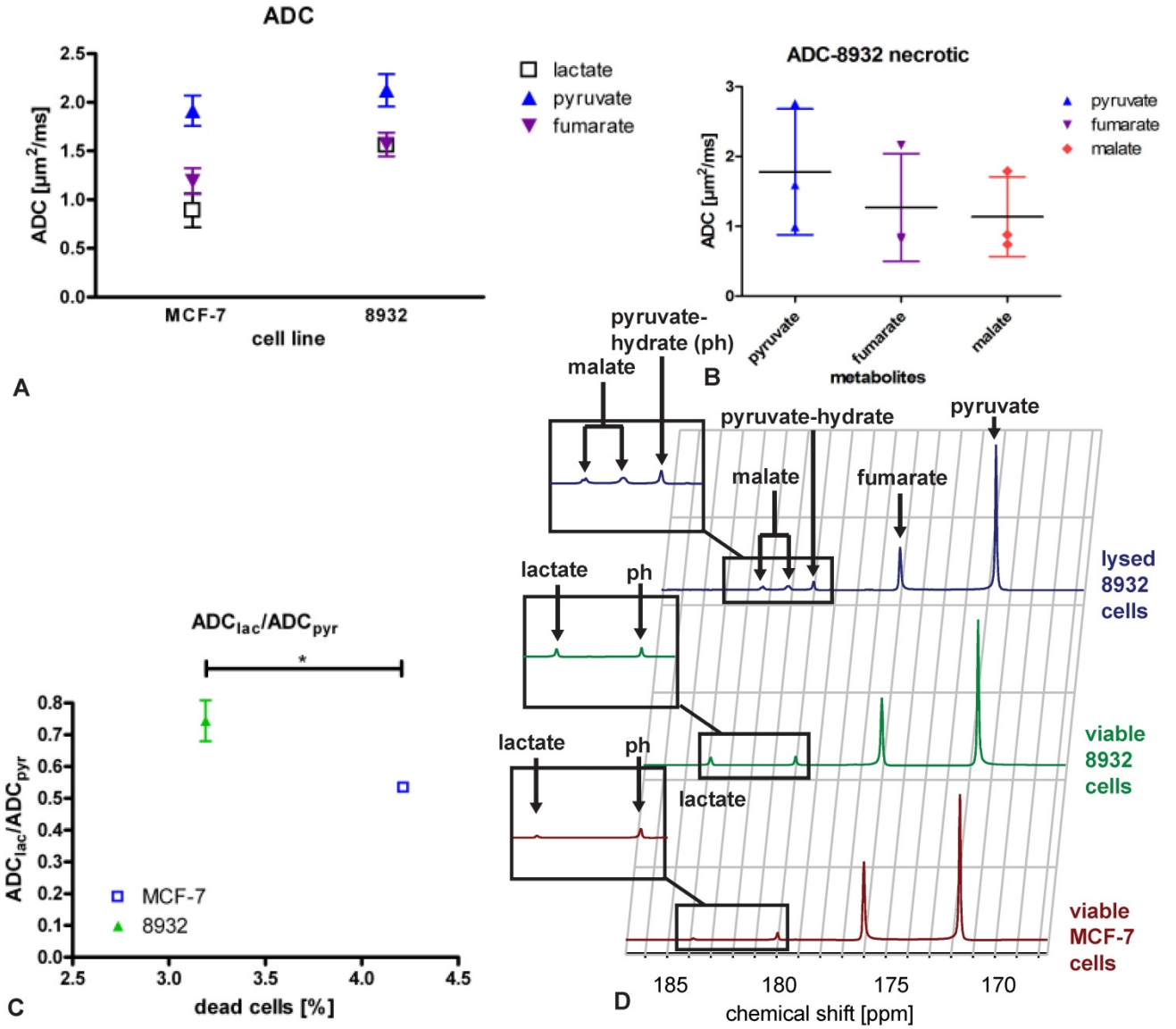

Figure 1. Mean ADCs of MCF-7 breast cancer cells and 8932 pancreatic cancer cells (A) of lactate (except for necrotic cells, for which no lactate was detectable), pyruvate, fumarate and malate (detectable for necrotic cells only) and (B) necrotic 8932 pancreatic cancer cells which were treated with membrane permeabilizing Triton X-100 displaying that malate is only present in necrotic cells while at the same time no lactate metabolism is detectable. The bar represents the mean. (C) ADC_{lac}/ADC_{pyr} ratio of MCF-7 breast cancer cells and 8932 pancreatic cancer cells relative to the amount of dead cells (%). Mean values of ADC_{lac}/ADC_{pyr} between MCF-7 (0.533 ± 0.015) and 8932 cells (0.744 ± 0.064) showed a significant difference ($p = 0.048$). D displays sample spectra of MCF-7 cells, 8932 cells and necrotic 8932 cells.

Proton diffusion has been used as marker for response-to-treatment analysis in tumors for more than a decade [31-33]. It is based on the observation that as cellular density increases the added tortuosity within the microenvironment reduces water mobility [34]. Following cytotoxic treatment of cancer cells the extracellular space increases whereas the intracellular space becomes smaller [34]. In contrast to protons, which are present in all tissue compartments, hyperpolarized lactate, directly after its formation from pyruvate, is a marker of intracellular origin in viable cells following pyruvate-to-lactate conversion inside the cell. Therefore, the ADC of lactate in combination with the detection of the ADC of pyruvate, may be a more sensitive marker than the ADC of protons for detecting changes in membrane permeability. In viable cells, lactate efflux in the cells over time will lead to an increase of the lactate ADC, approaching the ADC of pyruvate when present exclusively extracellular, therefore reporting on transport. Necrotic processes in cells that cause a blending of intra- and extracellular compartments could also lead to an increase in the lactate ADC and therefore has to be assessed independently. By employing an established method to measure necrosis through measurement of fumarate-to-malate conversion [23, 26, 32], we are able to rule out contributions from necrosis to ADC_{lac}/ADC_{pyr}. In viable 8932 cells and MCF-7 cells no fumarate-to-malate conversion was detectable providing direct proof of cell viability. In 8932 cells that were lysed and became necrotic, fumarate-to-malate conversion was detectable. The presence of malate shows mitochondrial damage as the mitochondrial membrane gets disrupted and fumarate can hence be metabolized to malate by cytosolic fumarate hydratase. In these cells, no lactate formation was measured mainly due to a complete destruction of the cells and the resulting dilution of LDH and NADH. By co-polarization of pyruvate and fumarate we can therefore assess the cells' viability.

For the case of diffuse necrosis, the amount of malate being produced and the ADC_{lac}/ADC_{pyr} ratio might indicate the amount of cell death being present. ADC measurements can potentially complement lactate/pyruvate ratios *in vivo* in tumors to improve localization of necrotic areas and to assess whether wash-out of the fumarate hydratase took place.

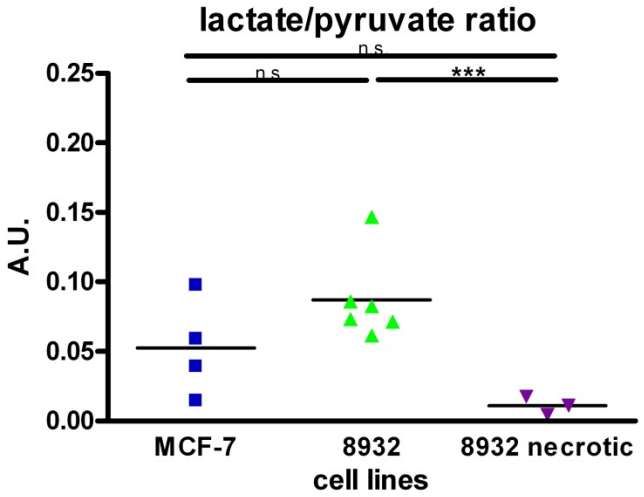

Figure 2. Pyruvate to lactate ratio in MCF-7, 8932 and necrotic cell lines as assessed by the specific spectra. The lactate to pyruvate ratio was higher in 8932 cells compared with MCF-7 and 8932 necrotic cells. Data are shown as single point observations, the bar represents the mean of the respective values. *** indicates a $p < 0.001$; n.s. = non significant difference as assessed by an ANOVA analysis.

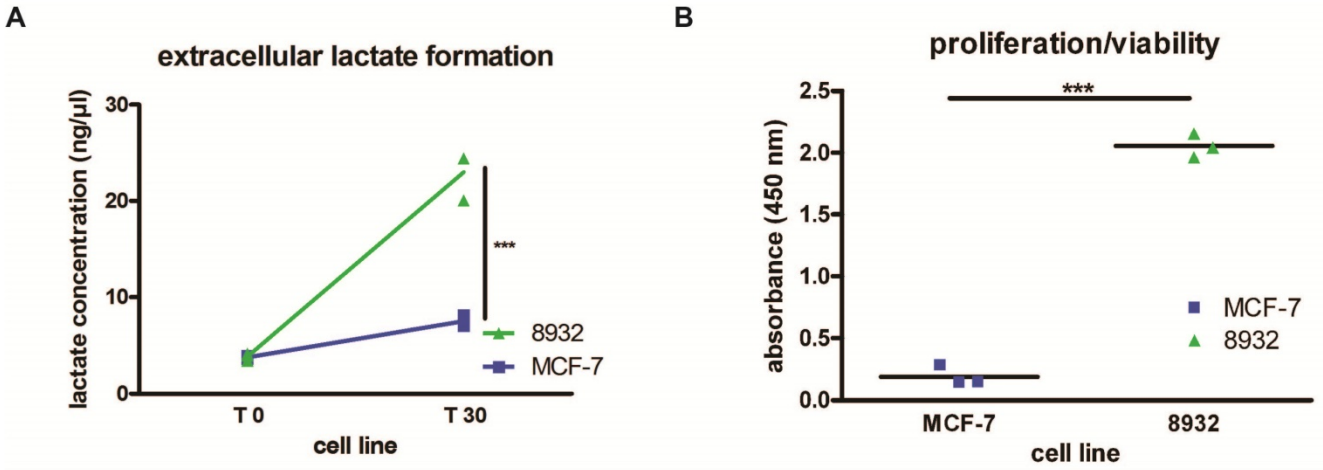

Figure 3. (A) 8932 pancreatic cancer cells show more lactate concentration in the medium thus displaying higher metabolic turnover compared to MCF-7 cells after addition of a 100 mM pyruvate solution and sample collection after 30 seconds (T30) ($p < 0.0001$; $n = 3$). T 0 displays lactate concentration in a steady-state prior to addition of pyruvate. (B) Absorbance measurements using a WST-1 proliferation/viability assay displaying higher proliferation/viability after 24 h in 8932 cells compared to MCF-7 cells ($p < 0.0001$; $n = 3$). The bar represents the mean.

We have demonstrated that the ADC_{lac}/ADC_{pyr} ratio is a biomarker to pick up differences in lactate export between the two cell lines MCF-7 and pancreatic cancer cells 8932, where increased export leads to an increase in ADC_{lac} and therefore to a relative increase of ADC_{lac}/ADC_{pyr}. Increased lactate export was further substantiated by an *in vitro* lactate assay, which showed statistically significant differences in the extracellular lactate concentrations of MCF-7 and 8932 cells. The two different time points in our *in vitro* setup were chosen analogously to the measurements in the NMR spectrometer in which pyruvate addition was followed by an incubation period of 30 seconds. Differences in lactate/pyruvate ratios from b = 0 points also revealed a clear trend with a higher ratio in 8932 cells compared to MCF-7 cells. In 8932 cells that were treated with Triton X-100, lactate-to-pyruvate ratio significantly decreased compared to 8932 cells, indicating that no additional lactate was produced as a consequence of the breakdown of the intracellular metabolism of the tumor cell (Figure 2).

With the introduction of the ADC ratio of lactate to pyruvate (ADC_{lac}/ADC_{pyr}), a measure of the difference between lactate and pyruvate diffusion restriction is accessible. Indirectly, this serves as a measure of lactate export. This roots in the observation that extracellular accumulation of lactate after rapid export from within the cell results in an increase in ADC_{lac}/ADC_{pyr}. It was shown previously, that in cells and animals ADC values of pyruvate are relatively high compared with ADC values of lactate, presumably because it was mainly extracellular whereas lactate was predominantly intracellular [4, 35-38].

Evaluation of the $T_{1,eff}$ of pyruvate and lactate did not show differences between lysed and normal cells pointing to the fact that the compartmental differences from different T_1s of the metabolites in extra- and intracellular compartments do not have to be taken into account for the analysis of these data (see also Table 1 and figure S1, supplementary material).

As a biological marker of cell proliferation/viability results obtained with the WST-1 assay showed also higher proliferation/viability in pancreatic cancer 8932 cells indicating a more aggressive tumor type. In previous studies it was shown that elevated lactate dehydrogenase enzyme concentrations in combination with alkaline phosphatase in the serum of patients suffering from resectable pancreatic ductal adenocarcinoma correlates with poor prognosis [39]. This is in accordance with our observation of elevated lactate level in 8932 cells which at the same time correlated with elevated ADC_{lac}/ADC_{pyr} ratios.

With regard to the second tumor cell type that we investigated, MCF-7, which is a human breast cancer cell line, it was previously shown that these cells do not upregulate MCT1 or MCT4 isoforms under hypoxic conditions but still show increased lactate concentrations [40]. This is in line with our observation in which we observed relatively low ADC_{lac}/ADC_{pyr} ratios in MCF-7 cells that correlated also with the low extracellular lactate concentrations from a biological conventional assay. Elevated extracellular lactate concentrations are notably of interest based on the fact that metastatic potential and tumor aggressiveness are correlated with it [10-13]. The clinical relevance of lactate content in tumor tissue has been also investigated in various human head and neck squamous cell carcinoma cell lines in which lactate content was determined non-invasively by proton magnetic resonance spectroscopy imaging showing that high turnover of pyruvate into lactate positively correlated with elevated radioresistance [41]. Discrimination of cell subtypes with different biological features such as lactate by non-invasive techniques might also help to further understand mechanisms by which certain cancer types escape or evade therapeutic approaches. Further studies have to be conducted in order to translate these first observations into solid *in vivo* data.

In conclusion, we have demonstrated for the first time that hyperpolarized ^{13}C diffusion-weighted spectroscopy using co-polarized pyruvate and fumarate *in vitro* is feasible. This combination can provide information about lactate efflux, about the viability and the state of necrosis of tumor cells. Therefore, our results point out new opportunities to characterize tumor cells beyond morphological characterization. Translation of this approach to *in vivo* models using spatially resolved diffusion imaging sequences seems promising for metabolic characterization of tumors [42].

Supplementary Material

Fig. S1. http://www.jcancer.org/v08p3078s1.pdf

Acknowledgements

We appreciated discussions with Steffen Glaser and Angela Otto. We thank the Bavarian NMR Centre for access to the NMR spectrometer and GE Global Research Europe for granting access to the hyperpolarizer. We acknowledge support from EU Grant No. 294582 (MUMI), BMBF (FKZ 13EZ1114), and DFG (SFB 824). G.S. is supported by the Deutsche Forschungsgemeinschaft (SFB824/C9) and the DKTK Joint Funding Program.

Competing Interests

The authors have declared that no competing interest exists.

References

1. Bhujwalla ZM, Artemov D, Ballesteros P, Cerdan S, Gillies RJ, Solaiyappan M. Combined vascular and extracellular pH imaging of solid tumors. NMR Biomed. 2002; 15: 114-9.
2. Terpstra M, High WB, Luo Y, de Graaf RA, Merkle H, Garwood M. Relationships among lactate concentration, blood flow and histopathologic profiles in rat C6 glioma. NMR Biomed. 1996; 9: 185-94.
3. Gatenby RA, Gillies RJ. Why do cancers have high aerobic glycolysis? Nat Rev Cancer. 2004; 4: 891-9.
4. Schilling F, Duwel S, Kollisch U, Durst M, Schulte RF, Glaser SJ, et al. Diffusion of hyperpolarized (13) C-metabolites in tumor cell spheroids using real-time NMR spectroscopy. NMR in biomedicine. 2013; 26: 557-68.
5. Halestrap AP, Price NT. The proton-linked monocarboxylate transporter (MCT) family: structure, function and regulation. The Biochemical journal. 1999; 343(Pt 2): 281-99.
6. Halestrap AP. Monocarboxylic acid transport. Comprehensive Physiology. 2013; 3: 1611-43.
7. Pinheiro C, Longatto-Filho A, Azevedo-Silva J, Casal M, Schmitt FC, Baltazar F. Role of monocarboxylate transporters in human cancers: state of the art. J Bioenerg Biomembr. 2012; 44: 127-39.
8. Baltazar F, Pinheiro C, Morais-Santos F, Azevedo-Silva J, Queiros O, Preto A, et al. Monocarboxylate transporters as targets and mediators in cancer therapy response. Histol Histopathol. 2014; 29: 1511-24.
9. Pertega-Gomes N, Baltazar F. Lactate transporters in the context of prostate cancer metabolism: what do we know? Int J Mol Sci. 2014; 15: 18333-48.
10. Stern R, Shuster S, Neudecker BA, Formby B. Lactate stimulates fibroblast expression of hyaluronan and CD44: the Warburg effect revisited. Experimental cell research. 2002; 276: 24-31.
11. Martins SF, Amorim R, Viana-Pereira M, Pinheiro C, Costa RF, Silva P, et al. Significance of glycolytic metabolism-related protein expression in colorectal cancer, lymph node and hepatic metastasis. BMC Cancer. 2016; 16: 535.
12. Ganapathy V, Thangaraju M, Prasad PD. Nutrient transporters in cancer: relevance to Warburg hypothesis and beyond. Pharmacol Ther. 2009; 121: 29-40.
13. Walenta S, Mueller-Klieser WF. Lactate: mirror and motor of tumor malignancy. Semin Radiat Oncol. 2004; 14: 267-74.
14. Kennedy BW, Kettunen MI, Hu DE, Brindle KM. Probing lactate dehydrogenase activity in tumors by measuring hydrogen/deuterium exchange in hyperpolarized l-[1-(13)C,U-(2)H]lactate. J Am Chem Soc. 2012; 134: 4969-77.
15. Van Zijl PC, Moonen CT, Faustino P, Pekar J, Kaplan O, Cohen JS. Complete separation of intracellular and extracellular information in NMR spectra of perfused cells by diffusion-weighted spectroscopy. Proceedings of the National Academy of Sciences of the United States of America. 1991; 88: 3228-32.
16. Bremerich J, Colet JM, Giovenzana GB, Aime S, Scheffler K, Laurent S, et al. Slow clearance gadolinium-based extracellular and intravascular contrast media for three-dimensional MR angiography. J Magn Reson Imaging. 2001; 13: 588-93.
17. Terreno E, Geninatti Crich S, Belfiore S, Biancone L, Cabella C, Esposito G, et al. Effect of the intracellular localization of a Gd-based imaging probe on the relaxation enhancement of water protons. Magnetic resonance in medicine. 2006; 55: 491-7.
18. Aime S, Caravan P. Biodistribution of gadolinium-based contrast agents, including gadolinium deposition. J Magn Reson Imaging. 2009; 30: 1259-67.
19. Reineri F, Daniele V, Cavallari E, Aime S. Assessing the transport rate of hyperpolarized pyruvate and lactate from the intra- to the extracellular space. NMR in biomedicine. 2016.
20. Hoehn-Berlage M. Diffusion-weighted NMR imaging: application to experimental focal cerebral ischemia. NMR in biomedicine. 1995; 8: 345-58.
21. Moseley ME, Cohen Y, Mintorovitch J, Chileuitt L, Shimizu H, Kucharczyk J, et al. Early detection of regional cerebral ischemia in cats: comparison of diffusion- and T2-weighted MRI and spectroscopy. Magnetic resonance in medicine. 1990; 14: 330-46.
22. Norris DG. The effects of microscopic tissue parameters on the diffusion weighted magnetic resonance imaging experiment. NMR in biomedicine. 2001; 14: 77-93.
23. Duwel S, Durst M, Gringeri CV, Kosanke Y, Gross C, Janich MA, et al. Multiparametric human hepatocellular carcinoma characterization and therapy response evaluation by hyperpolarized (13) C MRSI. NMR in biomedicine. 2016; 29: 952-60.
24. De Graaf RA. In vivo NMR spectroscopy : principles and techniques. 2nd ed. Chichester, West Sussex, England ; Hoboken, NJ: John Wiley & Sons; 2007.
25. Wilson DM, Keshari KR, Larson PE, Chen AP, Hu S, Van Criekinge M, et al. Multi-compound polarization by DNP allows simultaneous assessment of multiple enzymatic activities in vivo. J Magn Reson. 2010; 205: 141-7.
26. Gallagher FA, Kettunen MI, Hu DE, Jensen PR, Zandt RI, Karlsson M, et al. Production of hyperpolarized [1,4-13C2]malate from [1,4-13C2]fumarate is a marker of cell necrosis and treatment response in tumors. Proceedings of the National Academy of Sciences of the United States of America. 2009; 106: 19801-6.
27. Bard-Chapeau EA, Nguyen AT, Rust AG, Sayadi A, Lee P, Chua BQ, et al. Transposon mutagenesis identifies genes driving hepatocellular carcinoma in a chronic hepatitis B mouse model. Nat Genet. 2014; 46: 24-32.
28. von Burstin J, Eser S, Paul MC, Seidler B, Brandl M, Messer M, et al. E-cadherin regulates metastasis of pancreatic cancer in vivo and is suppressed by a SNAIL/HDAC1/HDAC2 repressor complex. Gastroenterology. 2009; 137: 361-71, 71 e1-5.
29. Eser S, Reiff N, Messer M, Seidler B, Gottschalk K, Dobler M, et al. Selective requirement of PI3K/PDK1 signaling for Kras oncogene-driven pancreatic cell plasticity and cancer. Cancer Cell. 2013; 23: 406-20.
30. Kambadakone A, Yoon SS, Kim TM, Karl DL, Duda DG, DeLaney TF, et al. CT perfusion as an imaging biomarker in monitoring response to neoadjuvant bevacizumab and radiation in soft-tissue sarcomas: comparison with tumor morphology, circulating and tumor biomarkers, and gene expression. AJR American journal of roentgenology. 2015; 204: W11-8.
31. Lodi A, Woods SM, Ronen SM. Treatment with the MEK inhibitor U0126 induces decreased hyperpolarized pyruvate to lactate conversion in breast, but not prostate, cancer cells. NMR Biomed. 2012.
32. Bohndiek SE, Kettunen MI, Hu DE, Brindle KM. Hyperpolarized (13)C spectroscopy detects early changes in tumor vasculature and metabolism after VEGF neutralization. Cancer research. 2012; 72: 854-64.
33. EI Khouli RH, Jacobs MA, Mezban SD, Huang P, Kamel IR, Macura KJ, et al. Diffusion-weighted Imaging Improves the Diagnostic Accuracy of Conventional 3.0-T Breast MR Imaging1. Radiology. 2010; 256: 64-73.
34. Galban CJ, Hoff BA, Chenevert TL, Ross BD. Diffusion MRI in early cancer therapeutic response assessment. NMR in biomedicine. 2016.
35. Sogaard LV, Schilling F, Janich MA, Menzel MI, Ardenkjaer-Larsen JH. In vivo measurement of apparent diffusion coefficients of hyperpolarized (1)(3)C-labeled metabolites. NMR in biomedicine. 2014; 27: 561-9.
36. Koelsch BL, Sriram R, Keshari KR, Leon Swisher C, Van Criekinge M, Sukumar S, et al. Separation of extra- and intracellular metabolites using hyperpolarized (13)C diffusion weighted MR. J Magn Reson. 2016; 270: 115-23.
37. Sriram R, Van Criekinge M, Hansen A, Wang ZJ, Vigneron DB, Wilson DM, et al. Real-time measurement of hyperpolarized lactate production and efflux as a biomarker of tumor aggressiveness in an MR compatible 3D cell culture bioreactor. NMR in biomedicine. 2015; 28: 1141-9.
38. Keshari KR, Sriram R, Koelsch BL, Van Criekinge M, Wilson DM, Kurhanewicz J, et al. Hyperpolarized 13C-pyruvate magnetic resonance reveals rapid lactate export in metastatic renal cell carcinomas. Cancer research. 2013; 73: 529-38.
39. Ji F, Fu SJ, Guo ZY, Pang H, Ju WQ, Wang DP, et al. Prognostic value of combined preoperative lactate dehydrogenase and alkaline phosphatase levels in patients with resectable pancreatic ductal adenocarcinoma. Medicine (Baltimore). 2016; 95: e4065.
40. Jamali S, Klier M, Ames S, Barros LF, McKenna R, Deitmer JW, et al. Hypoxia-induced carbonic anhydrase IX facilitates lactate flux in human breast cancer cells by non-catalytic function. Sci Rep. 2015; 5: 13605.
41. Quennet V, Yaromina A, Zips D, Rosner A, Walenta S, Baumann M, et al. Tumor lactate content predicts for response to fractionated irradiation of human squamous cell carcinomas in nude mice. Radiother Oncol. 2006; 81: 130-5.
42. Koelsch BL, Reed GD, Keshari KR, Chaumeil MM, Bok R, Ronen SM, et al. Rapid in vivo apparent diffusion coefficient mapping of hyperpolarized (13) C metabolites. Magnetic resonance in medicine. 2015; 74: 622-33.